SAND2022-16982C

IEEE International Conference on Rebooting Computing (ICRC 2022)
San Francisco, California, USA, December 8-9, 2022

Sandia National Laboratories

Ballistic Asynchronous Reversible Computing in Superconducting Circuits

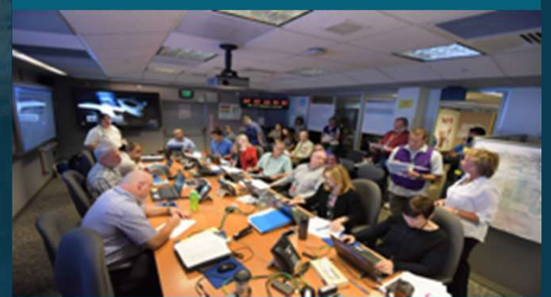

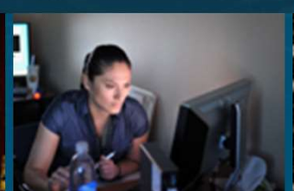

Thursday, December 8th, 2022

Michael P. Frank, Center for Computing Research

with Rupert Lewis (Quantum Phenomena Dept.)

Approved for public release, SAND2022-____ C

U.S. DEPARTMENT OF ENERGY | NNSA National Nuclear Security Administration

Sandia National Laboratories is a multimission laboratory managed and operated by National Technology & Engineering Solutions of Sandia, LLC, a wholly owned subsidiary of Honeywell International Inc., for the U.S. Department of Energy's National Nuclear Security Administration under contract DE-NA0003525.

Sandia National Laboratories is a multimission laboratory managed and operated by National Technology & Engineering Solutions of Sandia, LLC, a wholly owned subsidiary of Honeywell International Inc., for the U.S. Department of Energy's National Nuclear Security Administration under contract DE-NA0003525.

Abstract (hide during talk)

In recent years we have been exploring a novel asynchronous, ballistic physical model of reversible computing, variously termed ABRC (Asynchronous Ballistic Reversible Computing) or BARC (Ballistic Asynchronous Reversible Computing). In this model, localized information-bearing pulses propagate bidirectionally along nonbranching interconnects between I/O ports of stateful circuit elements, which carry out reversible transformations of the local digital state. The model appears suitable for implementation in superconducting circuits, using the naturally quantized configuration of magnetic flux in the circuit to encode digital information. One of the early research thrusts in this effort involves the enumeration and classification, at an abstract theoretical level, of the distinct possible reversible digital functional behaviors that primitive BARC circuit elements may exhibit, given the applicable conservation and symmetry constraints in superconducting implementations. In this paper, we describe the motivations for this work, outline our research methodology, and summarize some of the noteworthy preliminary results to date from our theoretical study of BARC elements for bipolarized pulses, and having up to three I/O ports and two internal digital states.

Contributors to our Reversible Computing research program

Sandia National Laboratories

- Full group of recent staff at Sandia:
  - Michael Frank (Cognitive & Emerging Computing)
  - Robert Brocato (RF MicroSystems) – now retired
  - David Henry (MESA Hetero-Integration)
  - Rupert Lewis (Quantum Phenomena)
    - Terence "Terry" Michael Bretz-Sullivan
  - Nancy Missert (Nanoscale Sciences) – now retired
    - Matt Wolak (now at Northrop-Grumman)
  - Brian Tierney (Rad Hard CMOS Technology)

Thanks are due to Sandia's LDRD program, DOE's ASC program, and the DoD/ARO ACI (Advanced Computing Initiative) for their support of this line of research!

- Thanks are also due to the following colleagues & external research collaborators:
  - Karpur Shukla (CMU → Flame U. → Brown U.)
    - Currently in Prof. Jimmy Xu's Lab for Emerging Techs.
  - Hannah Earley (Cambridge U. → startup)
  - Erik DeBenedictis (Sandia → Zettaflops, LLC)
  - Joseph Friedman (UT Dallas)
    - with A. Edwards, X. Hu, B.W. Walker, F. Garcia-Sanchezy, P. Zhou, J.A.C. Incorviaz, A. Paler
  - Kevin Osborn (LPS/JQI)
    - Liuqi Yu, Ryan Clarke, Han Cai
  - Steve Kaplan
  - Rudro Biswas (Purdue)
    - Dewan Woods & Rishabh Khare
  - Tom Conte (Georgia Tech/CRNCH)
    - Anirudh Jain, Gibran Essa
  - David Guéry-Odelin (Toulouse U.)
  - FAMU-FSU College of Engineering:
    - Sastry Pamidi (ECE Chair) & Jerris Hooker (Instructor)
    - 2019-20 students:
      - Frank Allen, Oscar L. Corces, James Hardy, Fadi Matloob
    - 2020-21 students:
      - Marshal Nachreiner, Samuel Perlman, Donovan Sharp, Jesus Sosa

Talk Abstract/Outline

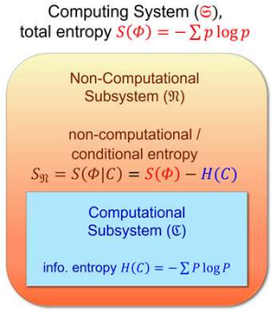

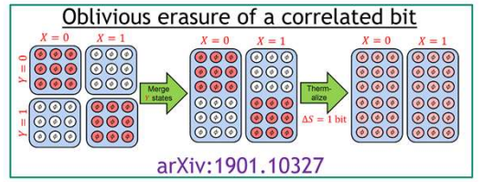

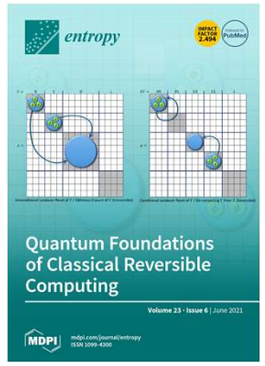

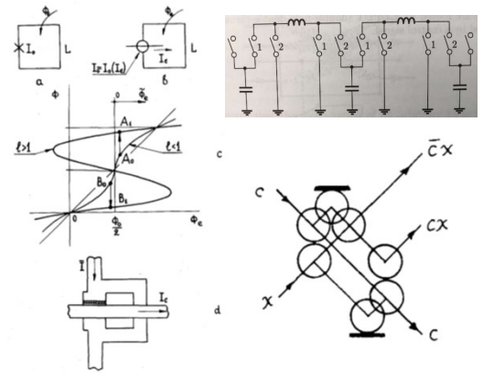

Ballistic Asynchronous Reversible Computing in Superconducting Circuits

- Background: *Why Reversible Computing*?
  - Relevant classic results in the thermodynamics of computing
    - Recently generalized to quantum case
  - Two major types of approaches to reversible computing in superconducting circuits:
    - *Adiabatic* approaches – Well-developed today.
      - Likharev's *parametric quantron* (1977); more recent QFP tech (YNU & collabs.) w. substantial demo chips.
    - *Ballistic* approaches – Much less mature to date.
      - Fredkin & Toffoli's early concepts (1978–'81); much more recent work at U. Maryland, Sandia, UC Davis
- **Review:** The relatively new *<u>asynchronous</u>* ballistic approach to RC in SCE.
  - Addresses concerns w instability of the synchronous ballistic approach
  - Potential advantages of asynchronous ballistic RC (vs. adiabatic approaches)
  - Implementation w. superconducting circuits (BARCS effort).
- **<u>Focus of this Talk:</u>**
  - Presenting our recent work on enumerating/classifying possible BARCS functions w. ≤3 ports and ≤2 states.

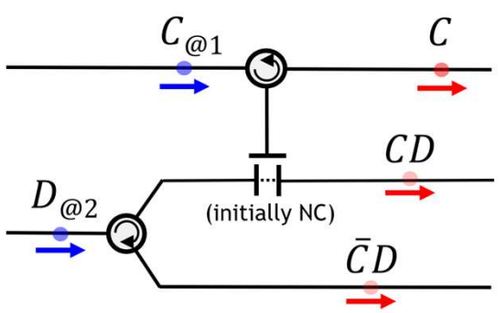

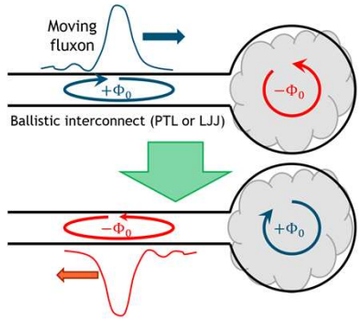

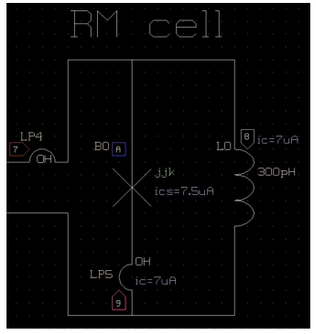

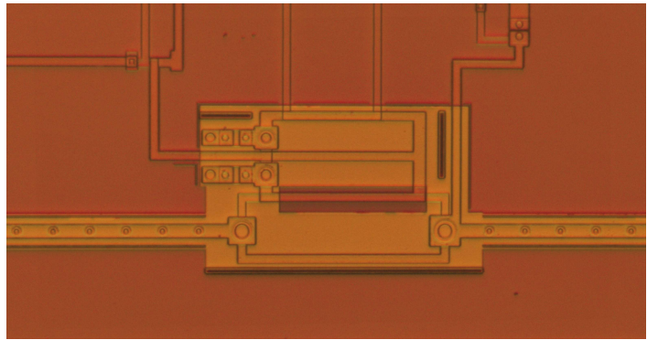

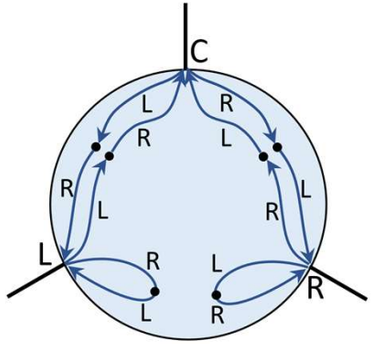

Why Reversible Computing?

Thermodynamics of computing: Relevant classic results

Based on the pioneering historical insights of Landauer & Bennett…

1. Fundamental Theorem of the Thermodynamics of Computing →
   - Unification of physical and information-theoretic entropy.
     - Implies interconvertibility of computational and non-computational entropy.

2. Landauer's Principle (proper) →
   - Loss of known/correlated computational information to a thermal environment transforms it into *new* physical entropy.

3. Conventional digital architectures (which discard correlated information all the time) have a *fundamental* efficiency limit…
   - $\geq kT \ln 2$ energy dissipation per bit of information loss.
     - Actual losses per bit erased in practical designs tend to be at least 10s–1000s of kT.

4. Alternative *reversible* digital architectures which transform states 1:1 can (at least in principle) avoid the Landauer limit.
   - There is no known fundamental efficiency limit for reversible machines.

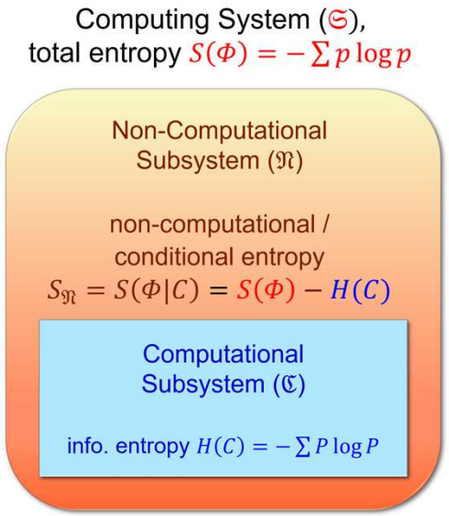

$$P(\boldsymbol{c}_j) = \sum_{\phi_i \in \boldsymbol{c}_j} p(\phi_i)$$

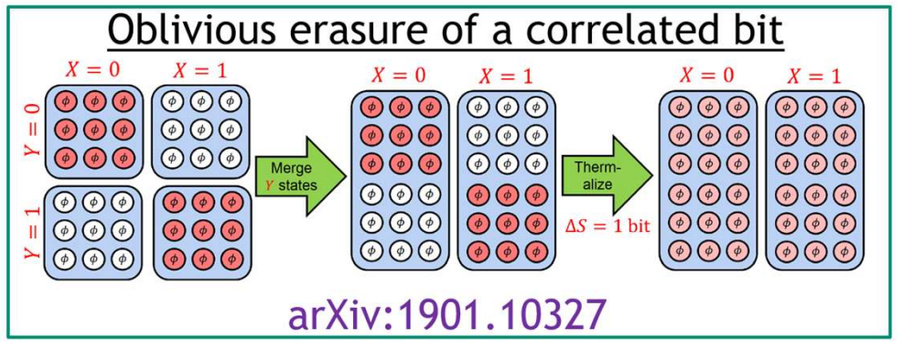

Quantum generalizations of classic results surveyed in M. Frank & K. Shukla, doi:10.3390/e23060701 –

Pendulum adiabatic processor (MIT '99)

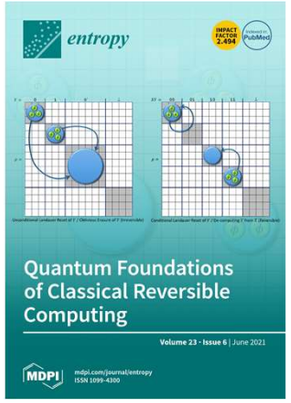

The two major approaches to reversible computing
Both relevant in superconducting electronics

10.1109/TMAG.1977.1059351:

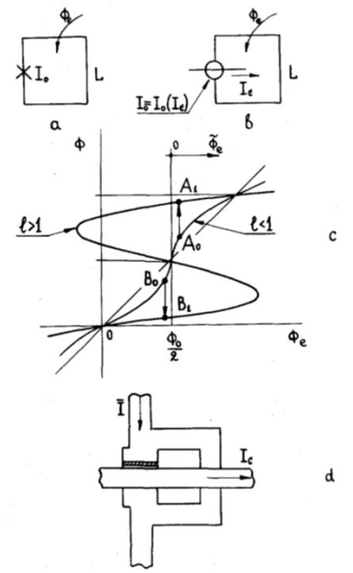

***Adiabatic* approaches** – based on *gradually* transforming a device's potential energy surface

- General method suggested in Landauer's original (1961) paper.
  - By definition, transitions are *slow* compared to the natural relaxation timescale of the device.
- First historical example of an engineered fully adiabatic electronic logic cell:
  - Likharev's *parametric quantron* (1977) – Use a *control current* I_c to raise/lower the potential energy barrier between loop states.
- Modern AQFP/RQFP technology from YNU has a similar spirit, but is much more well-developed.

***Ballistic* approaches** – based on *ballistic* dynamics & *elastic* interactions between DOFs

- Assumes relatively slight coupling between dynamical DOFs and the thermal environment…
  - Interactions happen *fast* relative to that coupling, so there isn't *time* for the dynamical excited state to relax thermally – dynamical energy largely *conserved* in the DOFs of interest.
- Early electronic & mechanical concepts proposed by Fredkin & Toffoli:
  - Early electronic concept (1978) as an underdamped LC circuit with idealized switches…
  - Simple mechanical thought experiment (1981)… "Billiard Ball Model"
- But, almost no engineering development of this approach from 1980 – 2010!
  - Why? The original concept appeared to have intractable issues w. synchronization / chaotic instabilities…

10.1007/978-1-4471-0129-1_2:

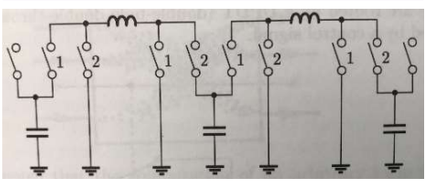

10.1007/BF01857727:

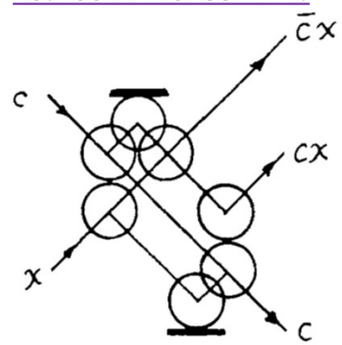

Ballistic Reversible Computing

Can we envision reversible computing as a *deterministic* elastic interaction process?

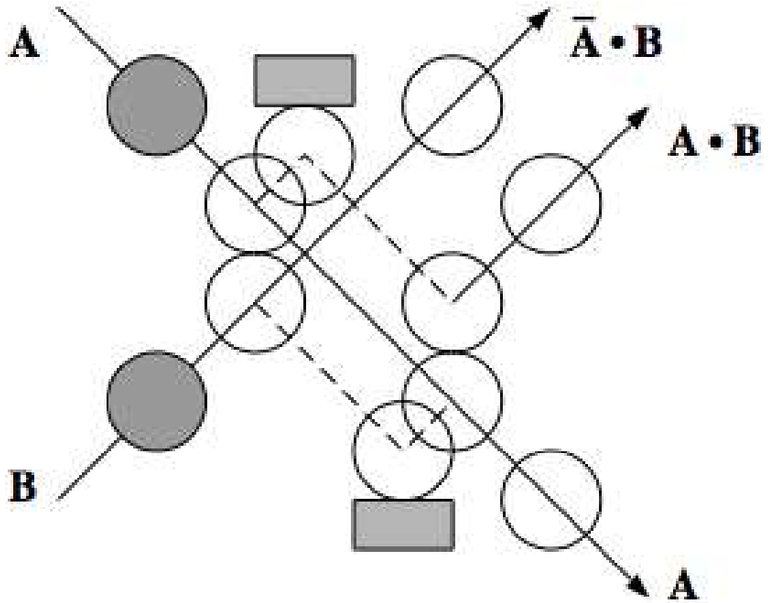

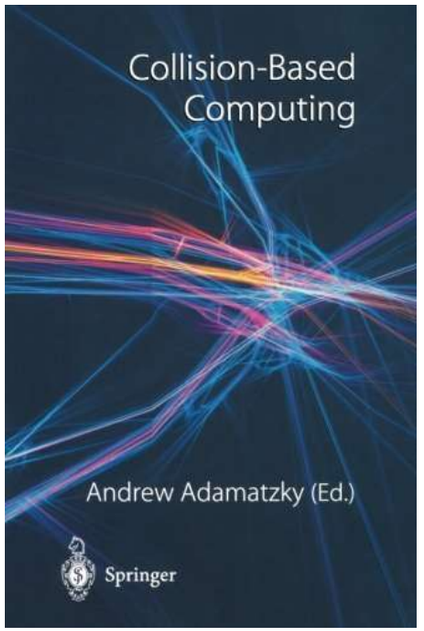

Historical origin of this concept:

- Fredkin & Toffoli's *Billard Ball Model* of computation ("Conservative Logic," IJTP 1982).
  - Based on elastic collisions between moving objects.
  - Spawned a subfield of "collision-based computing."
    - Using localized pulses/solitons in various media.

No power-clock driving signals needed!

- Devices operate when data signals arrive.
- The operation energy is carried by the signal itself.
  - Most of the signal energy is preserved in outgoing signals.

However, all (or almost all) of the existing design concepts for ballistic computing invoke implicitly *synchronized* arrivals of ballistically-propagating signals…

- Making this work in reality presents some serious difficulties, however:
  - Unrealistic in practice to assume precise alignment of signal arrival times.
    - Thermal fluctuations & quantum uncertainty, at minimum, are always present.
  - Any relative timing uncertainty leads to chaotic dynamics when signals interact.
    - Exponentially-increasing uncertainties in the dynamical trajectory.
  - Deliberate *re*synchronization of signals whose timing relationship is uncertain incurs an inevitable energy cost.

Can we come up with a new ballistic model that avoids these problems?

Ballistic Asynchronous Reversible Computing (BARC)

Problem: Conservative (dissipationless) dynamical systems generally tend to exhibit chaotic behavior…

- This results from direct nonlinear *interactions* between multiple continuous dynamical degrees of freedom (DOFs), which amplify uncertainties, exponentially compounding them over time…
  - *E.g.*, positions/velocities of ballistically-propagating "balls"
    - Or more generally, any localized, cohesive, momentum-bearing entity: Particles, pulses, quasiparticles, solitons…

Core insight: In principle, we can greatly reduce or eliminate this tendency towards dynamical chaos…

- We can do this simply by *avoiding* any direct interaction between continuous DOFs of different ballistically-propagating entities

Require localized pulses to arrive *asynchronously*—and furthermore, at clearly distinct, *non-overlapping* times

- Device's dynamical trajectory then becomes *independent* of the precise (absolute *and* relative) pulse arrival times
  - As a result, timing uncertainty per logic stage can now accumulate only *linearly*, not exponentially!
    - Only relatively occasional re-synchronization will be needed
- For devices to still be capable of doing logic, they must now maintain an internal discrete (digitally-precise) state variable—a stable (or at least metastable) stationary state, *e.g.*, a ground state of a well

No power-clock signals, unlike in adiabatic designs!

- Devices simply operate whenever data pulses arrive
- The operation energy is carried by the pulse itself
  - Most of the energy is preserved in outgoing pulses
    - Signal restoration can be carried out incrementally

Goal of current effort at Sandia: Demonstrate BARC principles in an implementation based on fluxon dynamics in SuperConducting Electronics (SCE)

(BARCS effort)

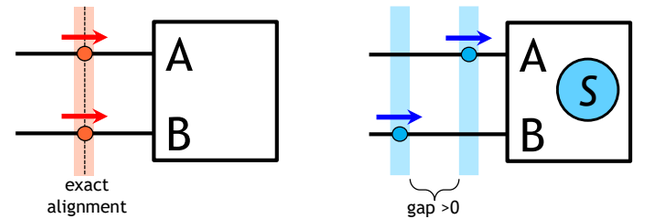

Synchronous Ballistic | Asynchronous Ballistic

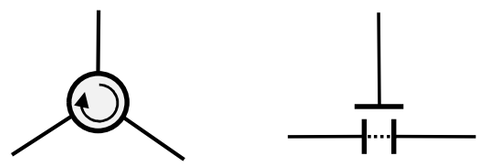

Rotary (Circulator) | Toggled Barrier

Example BARC device functions

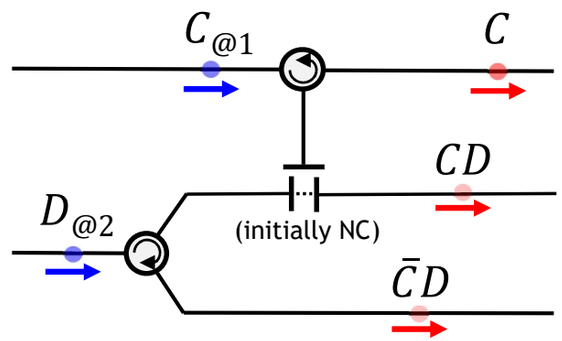

Example logic construction

Simplest Fluxon-Based (bipolarized) BARC Function

One of our early tasks: Characterize the simplest nontrivial BARC device functionalities, given a few simple design constraints applying to an SCE-based implementation, such as:

- (1) Bits encoded in fluxon polarity; (2) Bounded planar circuit conserving flux; (3) Physical symmetry.

Determined through theoretical hand-analysis that the simplest such function is the ***1-Bit, 1-Port Reversible Memory Cell (RM):***

- Due to its simplicity, this was then the preferred target for our subsequent detailed circuit design efforts…

RM Transition Table

Input Syndrome		Output Syndrome
+1(+1)	→	(+1)+1
+1(−1)	→	(+1)−1
−1(+1)	→	(−1)+1
−1(−1)	→	(−1)−1

RM icon:

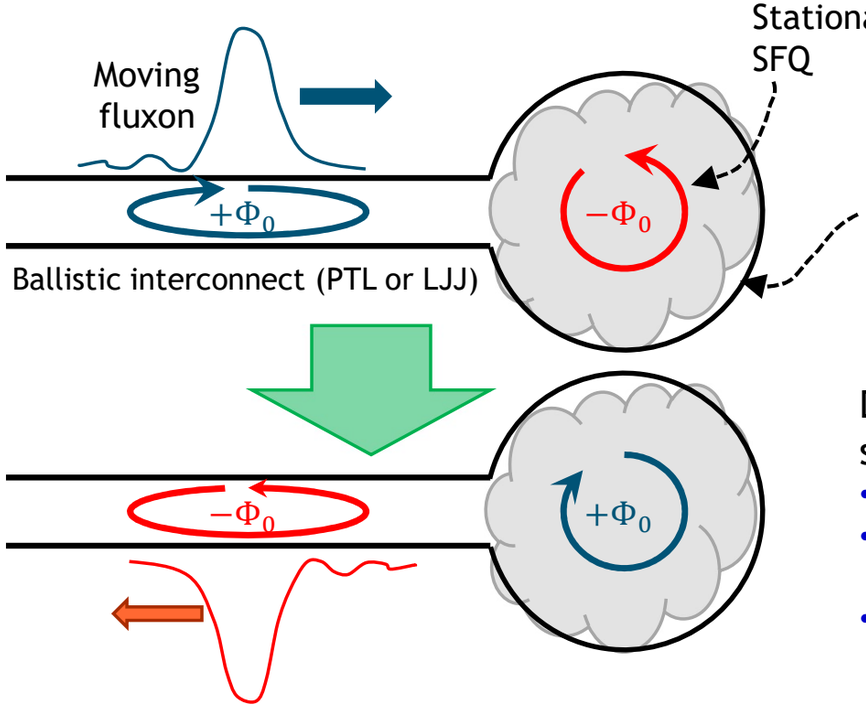

Some planar, unbiased, reactive SCE circuit w. a continuous superconducting boundary

- *Only* contains L's, M's, C's, and *unshunted* JJs
- Junctions should mostly be *subcritical* (avoids R_N)
- Conserves total flux, approximately nondissipative

Desired circuit behavior (NOTE: conserves flux, respects T symmetry & logical reversibility):

- If polarities are opposite, they are swapped (shown)
- If polarities are identical, input fluxon reflects back out with no change in polarity (not shown)
- *(Deterministic) elastic 'scattering'* type interaction: Input fluxon kinetic energy is (nearly) preserved in output fluxon

RM—First working (in simulation) implementation!

Erik DeBenedictis: "Try just strapping a JJ across that loop."
- This actually works!

"Entrance" JJ sized to = about 5 LJJ unit cells (~1/2 pulse width)
- I first tried it twice as large, & the fluxons annihilated instead…
  - "If a 15 μA JJ rotates by 2π, maybe ½ that will rotate by 4π" 🤔

Loop inductor sized so ±1 SFQ will fit in the loop (but not ±2)
- JJ is sitting a bit below critical with ± 1

WRspice simulations with ±1 fluxon initially in the loop
- Uses `ic` parameter, & `uic` option to `.tran` command
  - Produces initial ringing due to overly-constricted initial flux
    - Can damp w. small shunt *G*

Polarity mismatch → Exchange

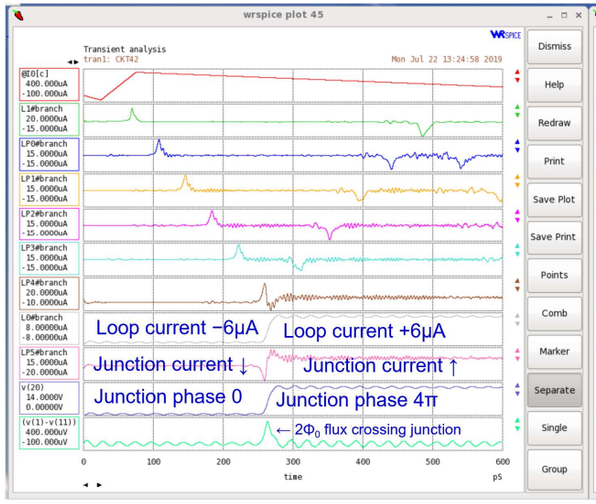

Polarity match → Reflect (=Exchange)

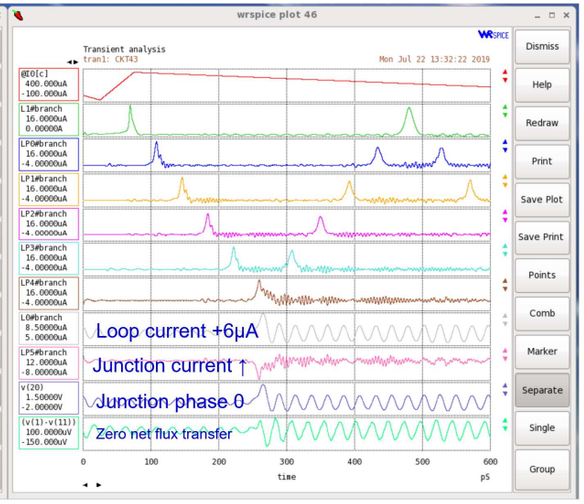

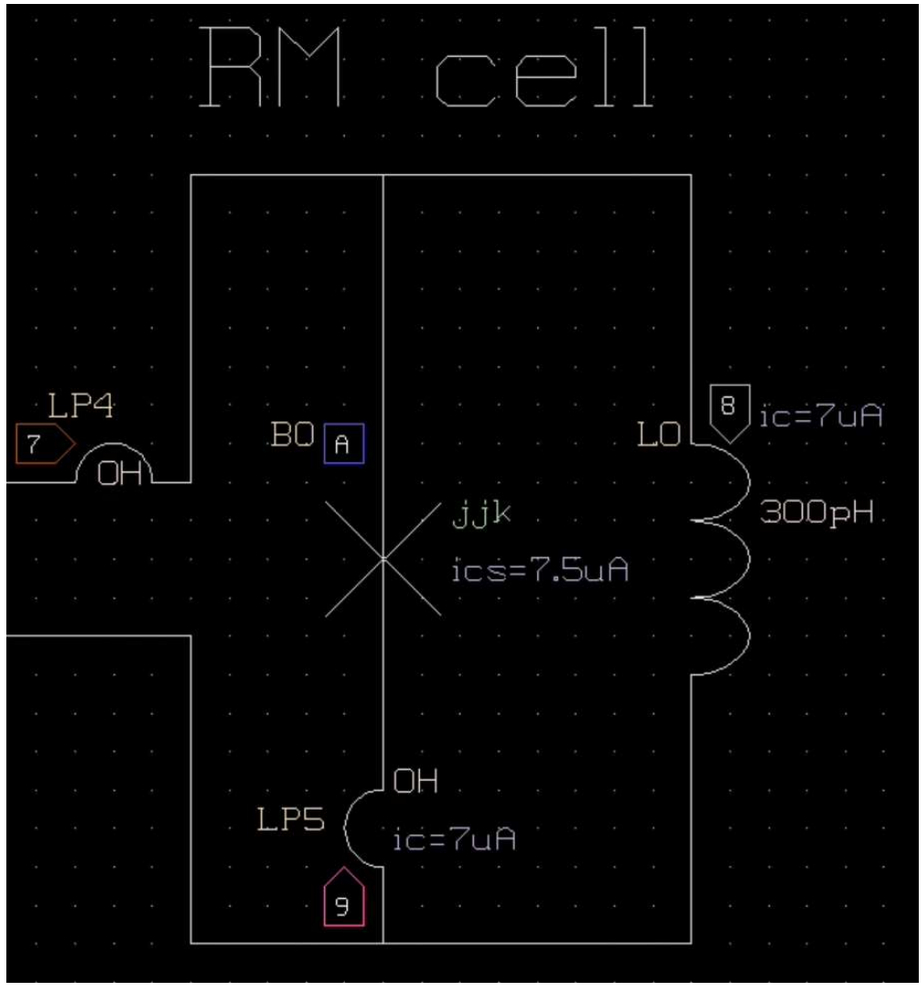

Resettable version of RM cell—Designed & Fabricated!

Apply current pulse of appropriate sign to flush the stored flux (the pulse here flushes out positive flux)

- To flush either polarity → Do both (±) resets in succession

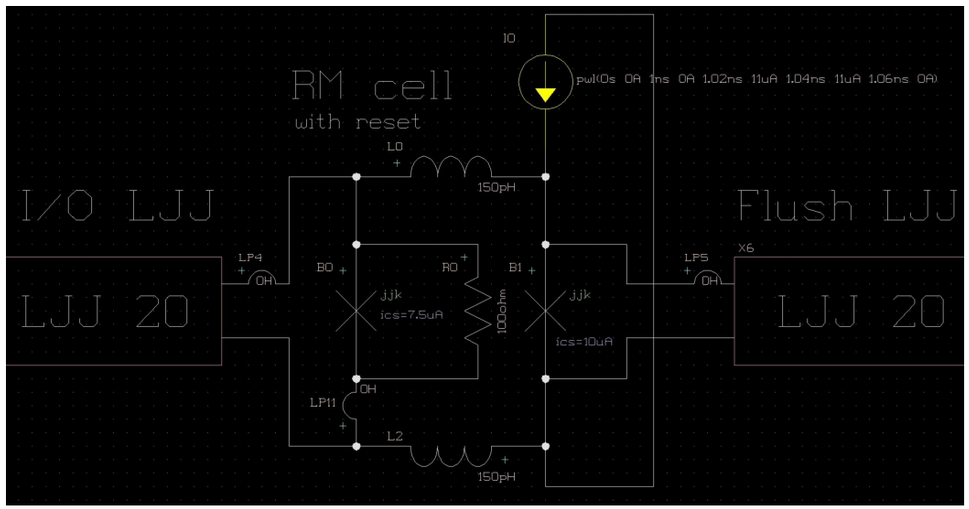

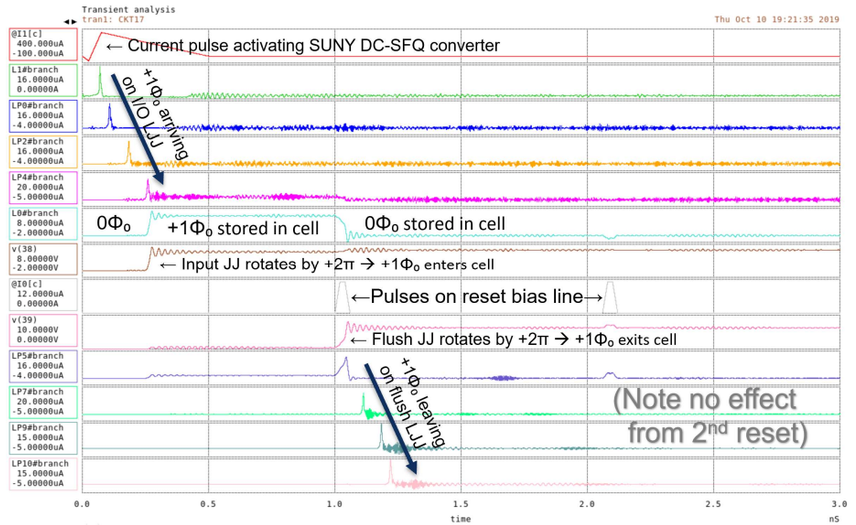

Fabrication at SeeQC with support from ACI

DC-SFQ & LJJ

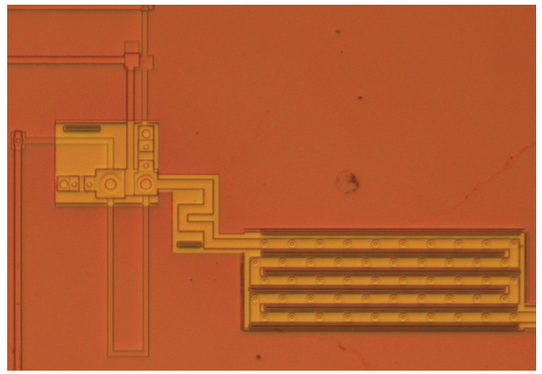

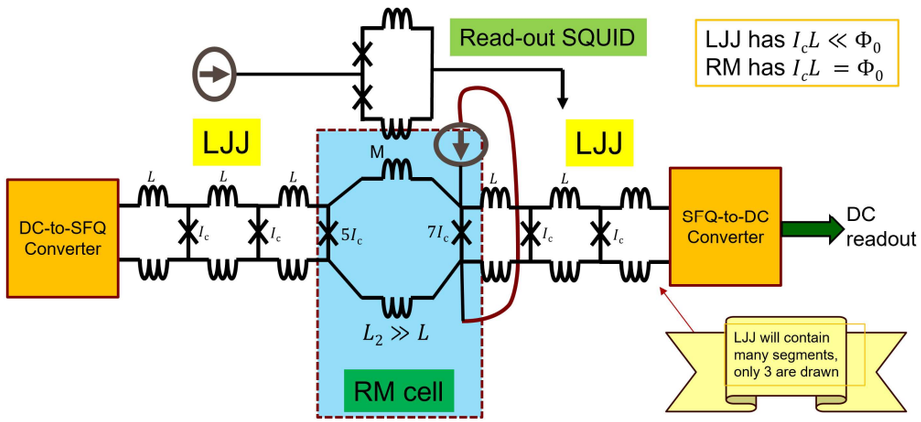

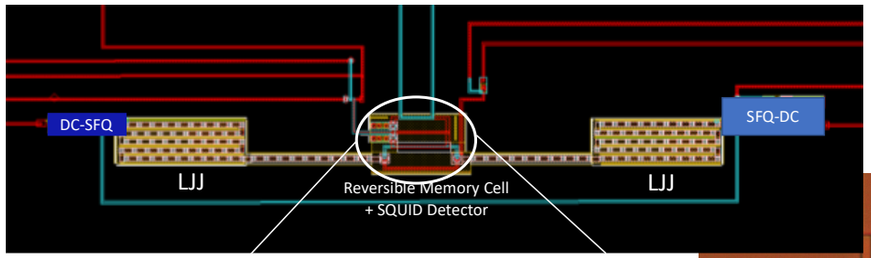

RM Cell & SQUID

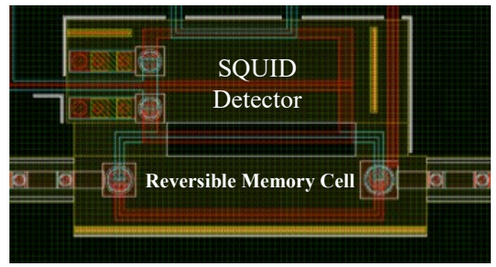

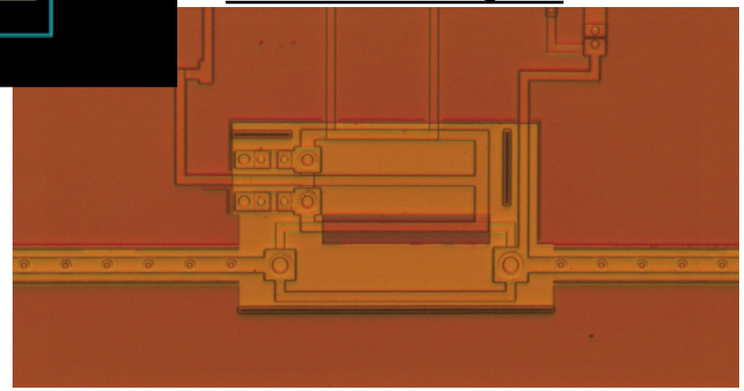

`barc` tool for enumerating/classifying BARCS device functions

Custom Python program with 16 modules.

Tool is now complete; will be open-sourced.

Layer-cake view of software architecture:

- Modules only import modules from lower-numbered layers.

Layer	Module Names & Descriptions
4	**barc** (top-level program)
3	**deviceType** – Classification of devices with given dimensions.
2	**deviceFunction** – Device with a specific transition function. **stateSet** – Identifies a set of accessible device states.
1	**pulseAlphabet** – Sets of pulse types. **pulseType** – Identifies a specific type of pulse. **state** – Identifies an internal state of a device. **symmetryGroup** – Equivalence class of device functions. **transitionFunction** – Bijective map, input→output syndromes.
0	**characterClass** – Defines a type of signal characters. **deviceDimensions** – Defines size parameters of devices. **dictPermuter** – Used to enumerate transition functions. **signalCharacter** – Identifies I/O event type (pulse type & port). **symmetryTransform** – Invertibly transforms a device function. **syndrome** – An initial or final condition for a device transition. **utilities** – Defines some low-level utility functions.

```
Symmetry group #38 has 6 functions:
    Function #155.
    Function #340.
    Function #481.
    Function #285.
    Function #365.
    Function #185.

Example: Function #155 = [1]*3(L,R):
    1(L) -> (R)2
    1(R) -> (L)3
    2(L) -> (R)1
    2(R) -> (R)3
    3(L) -> (L)2
    3(R) -> (L)1

Function #155 has the following symmetry properties:
    It is D-dual to function #481
    It is S-dual to function #481
    It is E(1,2)-dual to function #340
    It is E(1,3)-dual to function #185
    It is E(2,3)-dual to function #481
    It R(-1)-transforms to function #365
    It R(1)-transforms to function #285
```

← Example description of a symmetry-equivalence group as output by the `barc` tool.

Symmetry Relations of Interest

The following symmetry relations on BARC functions are considered in this work:

- ***Direction-reversal symmetry*** $\mathcal{D}$ –
  Symmetry under exchange of input & output syndromes (involution of transition func.)
- ***State-exchange symmetry*** $\mathcal{S}$ –
  Symmetry under an exchange of state labels (and fluxes, for flux-polarized states).
- ***Flux-negation symmetry*** $\mathcal{F}$ –
  Symmetry under negation of all (I/O flux & internal state) flux polarities.
- ***Moving-flux negation symmetry*** $\mathcal{M}$ – Symmetry under negation of all moving (I/O) flux polarities.
  - *Input flux negation symmetry* $\mathcal{I}$ – Symmetry under negation of all input flux polarities.
  - *Output flux negation symmetry* $\mathcal{O}$ – Symmetry under negation of all output flux polarities.
- ***Port-relabeling symmetries*** $\mathcal{R}_P$ – Symmetry under a particular permutation P of the port labels.
  - *Port exchange symmetry* $\mathcal{E}(p_i, p_j)$ – Symmetry wrt an exchange of labels between a particular pair of ports.
  - *Rotational symmetry* $\mathcal{R}_\mathrm{r}$ – Relevant for $n \geq 3$ ports. Symmetry under (planar) rotation of port labels.
  - *Reflection across port axis* $\mathcal{R}_{\{p_i\}}$ – Symmetry under reflection of ports on either side of port p_i.
  - *Mirror symmetry* $\mathcal{M}_2, \mathcal{M}_3$ – Symmetry under port exchange for a 2-port device, or any reflection for a rotationally symmetric 3-port device.
  - *Complete port symmetry* $\mathcal{R}(n)$ – Symmetry under *all* possible relabelings of the ports.

Equivalence Groups For the 24 One-Port, Two-State Elements:

$2 \cdot 1 \cdot 2 = 4$ I/O syndromes → $4! = 24$ permutations (raw reversible transition functions).

Stateful Reflector

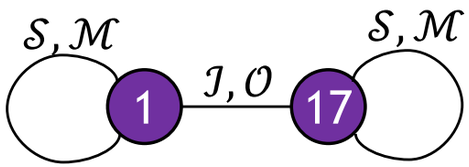

(State Unused—Not Atomic)

Configurable Inverter

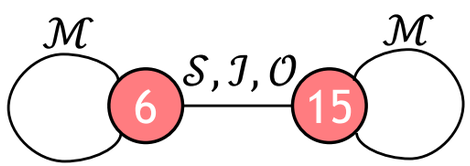

(Doesn't Change State)

Toggle

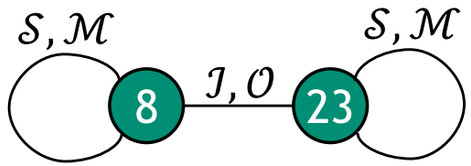

(Doesn't Use State)

Toggle & Conditional Invert

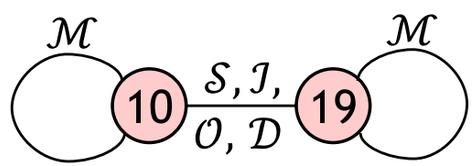

(Neither flux-negation symmetric nor flux-conserving)

Exchange (RM)

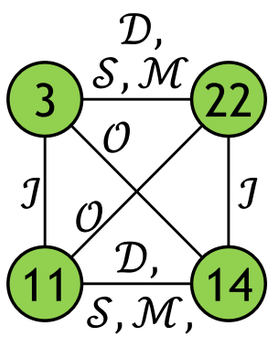

Conditional Toggle

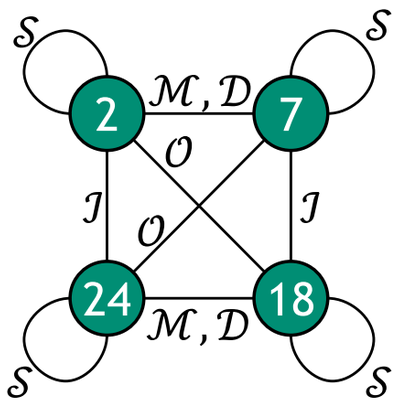

(Doesn't Use State)

Type 4

Type 5

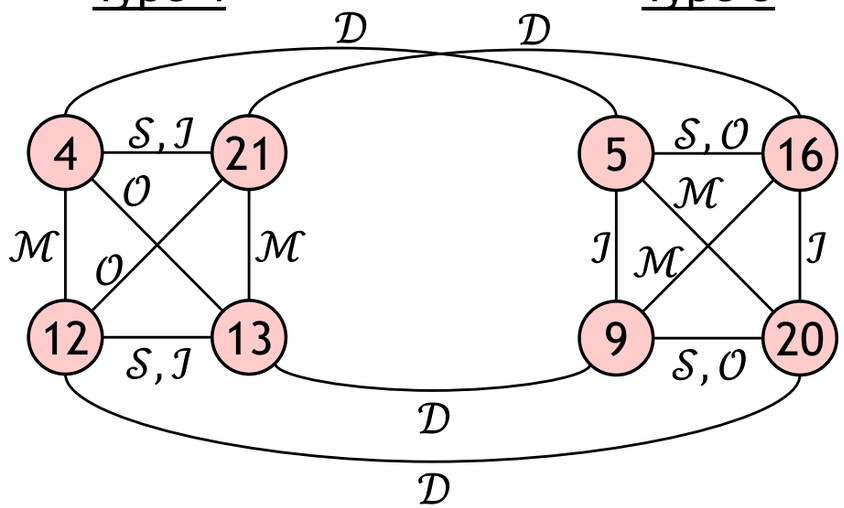

(Neither flux-negation symmetric nor flux-conserving)

Two-Port, Two-State, Flux-Polarized Elements

There are $2^3 = 8$ I/O syndromes, thus $8! = 40{,}320$ raw reversible transition functions.

- But only 96 of them satisfy the flux conservation constraint.
- And only 10 of these are nontrivial primitives satisfying all constraints.

These 10 functions sort into 7 equivalence groups as follows:

Self-Symmetry Group Size	Equivalence Group Size	Number of Equiv. Groups	Total # of Raw Trans. Funcs.
4	1	4	4
2	2	3	8
TOTALS:		**4**	**14**

The corresponding functional behaviors can be described as:

1. Reversible Shift Register (RSR)
2. Directed Reversible Shift Register (DRSR)
3. Filtering RM Cell (FRM)
4. Directed Filtering RM Cell (DFRM).
5. Polarized Flipping Diode (PFD).
6. Asymmetric Polarity Filter (APF).
7. Two-Port Reversible Memory Cell (RM2).

Illustrations of 2-port, 2-state, flux-polarized elements:

(Table Rows Shown for ↑ Initial State Only)

1. Reversible Shift Register (RSR):

Input syndrome	Output syndrome
↑⟩A(↑)	(↑)B⟩ ↑
↓⟩A(↑)	(↓)B⟩ ↑
↑⟩B(↑)	(↑)A⟩ ↑
↓⟩B(↑)	(↓)A⟩ ↑

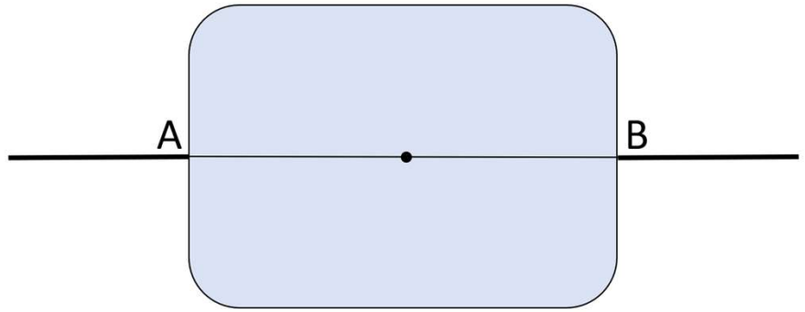

2. Directed Reversible Shift Register (DRSR):

Input syndrome	Output syndrome
↑⟩A(↑)	(↑)B⟩ ↑
↓⟩A(↑)	(↓)B⟩ ↑
↑⟩B(↑)	(↑)A⟩ ↑
↓⟩B(↑)	(↑)A⟩ ↓

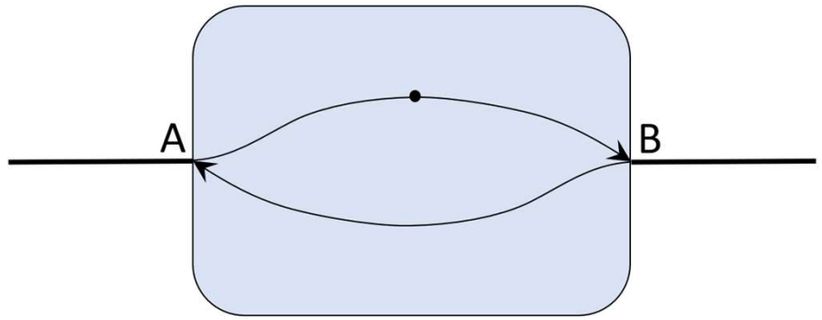

3. Filtering RM Cell (FRM):

Input syndrome	Output syndrome
↑⟩A(↑)	(↑)B⟩ ↑
↓⟩A(↑)	(↓)A⟩ ↑
↑⟩B(↑)	(↑)A⟩ ↑
↓⟩B(↑)	(↓)B⟩ ↑

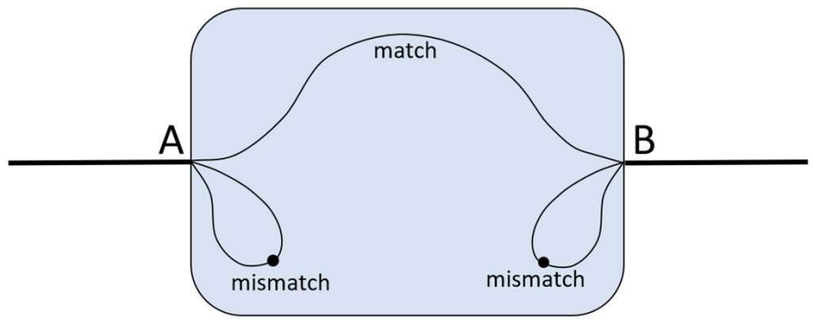

Illustrations of 2-port, 2-state, flux-polarized elements, cont.:

4. Directed Filtering RM Cell (DFRM):

Input syndrome	Output syndrome
↑⟩A(↑)	(↑)B⟩ ↑
↓⟩A(↑)	(↓)A⟩ ↑
↑⟩B(↑)	(↑)A⟩ ↑
↓⟩B(↑)	(↑)B⟩ ↓

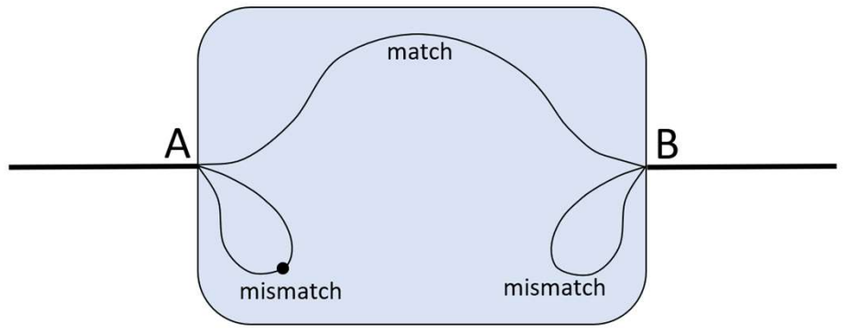

5. Polarized Flipping Diode (PFD):

Input syndrome	Output syndrome
↑⟩A(↑)	(↑)A⟩ ↑
↓⟩A(↑)	(↓)B⟩ ↑
↑⟩B(↑)	(↑)B⟩ ↑
↓⟩B(↑)	(↓)A⟩ ↑

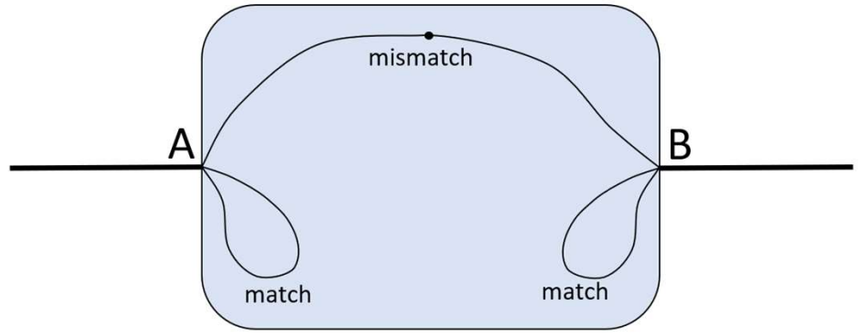

5. Asymmetric Polarity Filter (APF):

Input syndrome	Output syndrome
↑⟩A(↑)	(↑)A⟩ ↑
↓⟩A(↑)	(↓)B⟩ ↑
↑⟩B(↑)	(↑)B⟩ ↑
↓⟩B(↑)	(↑)A⟩ ↓

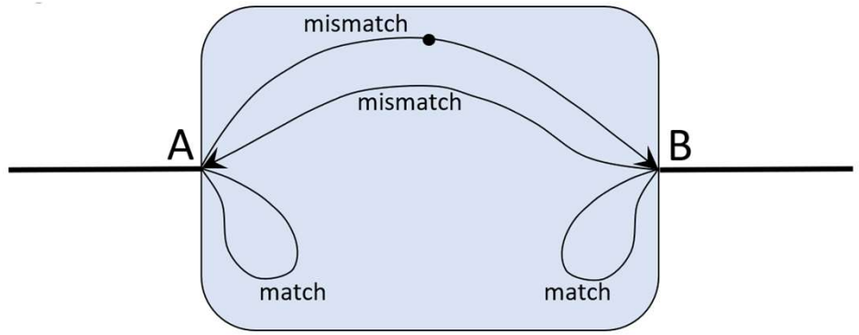

Two-Port, Two-State, Flux-Neutral Elements

There are $(2^2)! = 24$ raw flux-symmetric transition functions.

- 14 of these are nontrivial, atomic functional primitives.

These sort into 4 equivalence groups as follows:

Self-Symmetry Group Size	Equivalence Group Size	Number of Equiv. Groups	Total # of Raw Trans. Funcs.
4	2	3	6
1	8	1	8
TOTALS:		4	14

There are 5 distinct functional behaviors (described in forwards time direction):

1. **Alternating Barrier (AB)**, 2 reps. – See next slide.
2. **Polarized Flipping Diode (PFD)**, 2 reps..
3. **Variant Polarized Flipping Diode (VPFD)**, 2 reps..
4. **Asymmetric Polarized Flipping Diode (APFD)**, 4 reps.,
   ($\mathcal{D}$-dual to)
5. **Selectable Barrier (SD)**, 4 reps.

Ex. 2-port, 2-state neutral element: **Alternating Barrier (AB)**

Flux-conserving, flux-negation symmetric element.

- Also has mirror ($\mathcal{M}_2$) symmetry.
- Has two $\mathcal{D}$,$\mathcal{S}$ dual representations.

Flux-neutral internal states → Doesn't change fluxon polarity.

State descriptions:

- S^{+W}_{-B}: *Positive-wire, negative-barrier.*
  - Transmits positive (↑) fluxons, reflects negative (↓) fluxons.
- S^{+B}_{-W}: *Positive-Barrier, negative-wire.*
  - Reflects positive (↑) fluxons, transmits negative (↓) fluxons.

Transition function description:

- Fluxons arriving at either port are routed as per the state descriptions above.
- State toggles with every interaction.

Input Syndrome	Output Syndrome
$\uparrow\rangle p_1(S^{+W}_{-B})$	$(S^{+B}_{-W})p_2\rangle\uparrow$
$\downarrow\rangle p_1(S^{+W}_{-B})$	$(S^{+B}_{-W})p_1\rangle\downarrow$
$\uparrow\rangle p_2(S^{+W}_{-B})$	$(S^{+B}_{-W})p_1\rangle\uparrow$
$\downarrow\rangle p_2(S^{+W}_{-B})$	$(S^{+B}_{-W})p_2\rangle\downarrow$
$\uparrow\rangle p_1(S^{+B}_{-W})$	$(S^{+W}_{-B})p_1\rangle\uparrow$
$\downarrow\rangle p_1(S^{+B}_{-W})$	$(S^{+W}_{-B})p_2\rangle\downarrow$
$\uparrow\rangle p_2(S^{+B}_{-W})$	$(S^{+W}_{-B})p_2\rangle\uparrow$
$\downarrow\rangle p_2(S^{+B}_{-W})$	$(S^{+W}_{-B})p_1\rangle\downarrow$

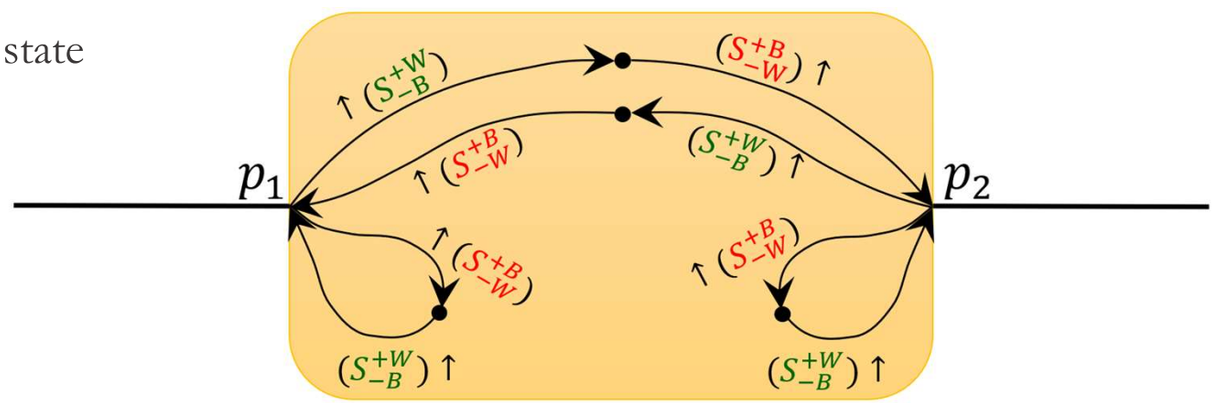

Results for Three-Port, Two-State Elements:

Devices with flux-polarized states:

- $2 \cdot 3 \cdot 2 = 12$ I/O syndromes
- $12! = 497{,}001{,}600$ raw reversible funcs.
- 25,920 of these are flux-conserving.
- 288 of those are flux-negation symmetric.
- 245 of those are atomic (primitives).
- 219 of those use the state non-trivially.
- Sort into 39 equiv. groups as follows →

Equivalence Class Size:	**1**	**2**	**3**	**6**	**12**	
Self-Symmetry Group Size:	**12**	**6**	**4**	**2**	**1**	**Tot.**
No. of Equivalence Classes:	1	4	6	24	4	**39**
Total number of Functions:	1	8	18	144	48	**219**

Devices with flux-neutral states:

- $1 \cdot 3 \cdot 2 = 6$ I/O syndromes (for ↑ inputs)
- $6! = 720$ permutations.
- 653 of them are atomic primtives.
- 600 of those use the state non-trivially.
- Sort into 45 equiv. groups as follows:

Equivalence Class Size:	**2**	**4**	**6**	**12**	**24**	
Self-Symmetry Group Size:	**12**	**6**	**4**	**2**	**1**	**Tot.**
No. of Equivalence Classes:	1	1	9	23	11	**45**
Total number of Functions:	2	4	54	276	264	**600**

Illustrations of some 3-port, 2-state flux-neutral elements

Recall there are 45 different non-trivial, atomic functional behaviors (counting $\mathcal{D}$-duals as equivalent).

Only a few exemplar behaviors are illustrated here.

Still seeking implementations of all these.

Polarized Neutral Toggle Rotary

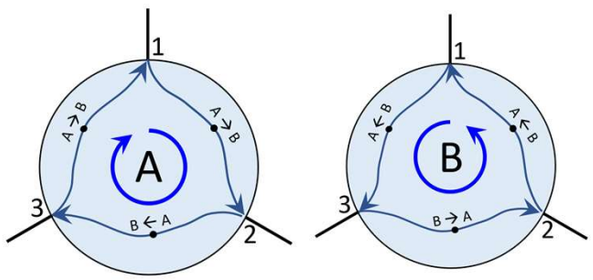

Behavior in Positive-Clockwise State (A)

Behavior in Positive-Counterclockwise State (B)

Polarized Controlled Flipping Diode

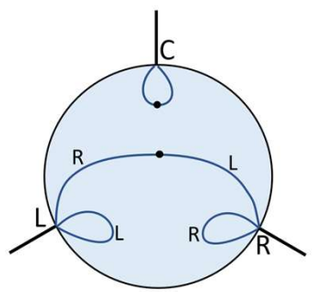

Polarized Throw Switch (Type A)

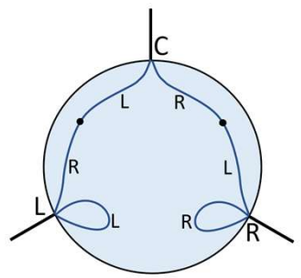

Polarized Throw Switch (Type B)

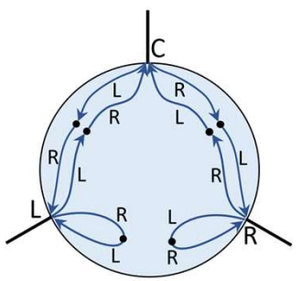

Polarized Toggle Controlled Barrier

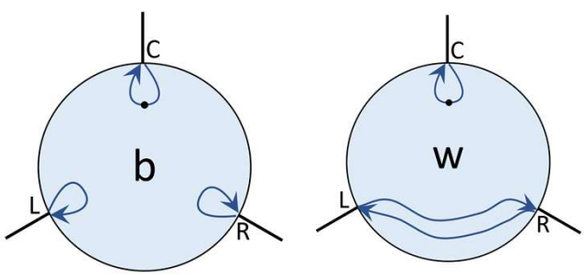

Behavior in Positive Barrier State (b)

Behavior in Positive Wire State (w)

Polarized Knock-Twice Toggle Controlled Barrier

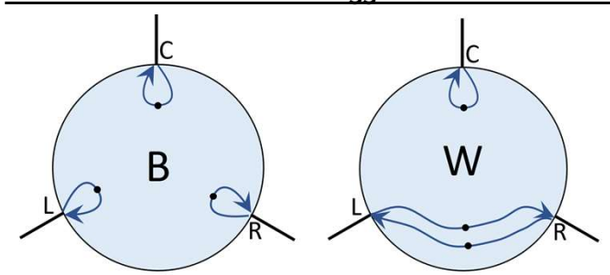

Behavior in Positive Barrier State (B)

Behavior in Positive Conducting State (W)

(All state behaviors shown are for + fluxons only; – fluxons interact oppositely w states)

Some Next Steps for the BARCS effort

1. Document classification results more fully.
2. Finish developing **SCIT** (Superconducting Circuit Innovation Tool) tool to facilitate discovery of circuit-level implementations of BARCS functions.
3. Better understand role of physical symmetries in the circuit design of BARCS elements.
4. Identify a computation-universal set of primitive elements that we also know how to implement!
5. Additional work on fabrication & empirical validation of BARCS circuit designs.
6. Understand the limits of energy efficiency of this approach.

Much work remains to be done!

- We would be very happy to recruit new collaborators

Conclusion

The long-neglected *ballistic* mode of reversible computing has recently attracted renewed interest.

- Classic problems with synchronization & chaotic instability in ballistic computing schemes seem to be resolvable via the asynchronous approach.
- Method appears to hold promise for achieving improved energy-delay products vs. adiabatic approaches.

Also, note that ballistic approaches are not viable at all in CMOS!

- CMOS has nothing like a ballistic flux soliton, & has no nonlinear reactive elements like JJs…
- Thus, we are leveraging unique advantages of superconducting electronics in this approach.

In this paper & talk, we reported our progress on enumerating & classifying possible BARCS functions…

- assuming logical reversibility, flux conservation, & flux negation symmetry.

Multiple US-based research groups in superconductor physics & engineering are now making early progress along this line of work…

- We invite additional domestic & international colleagues to join us in investigating this interesting line of research!

Ballistic Shift Registers

Work by Osborn & Wustmann, arxiv:2201.12999

First working multi-port elements in the BARCS paradigm!

- A type of two-port RM cell in which the output fluxon emerges from th port opposite the input. (Left-right symmetric.)

Work includes detailed simulation & analysis of circuit dynamics.

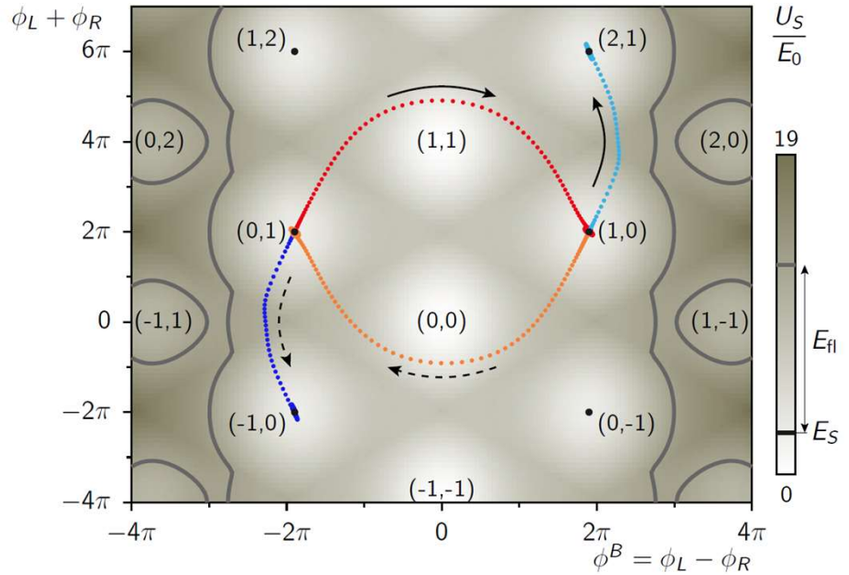

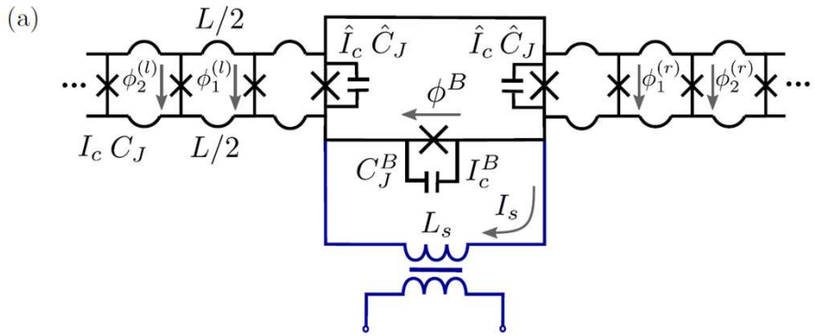

(b)

initial		final	
S	σ	S'	σ'
1	1	1	1
1	-1	-1	1
-1	1	1	-1
-1	-1	-1	-1

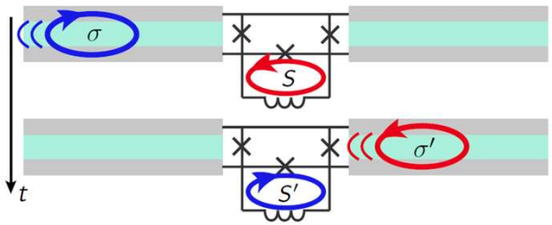

(c)

initial		final	
S	σ	S'	σ'
–	–	–	–
–	1	1	–
1	–	–	1
1	1	1	1

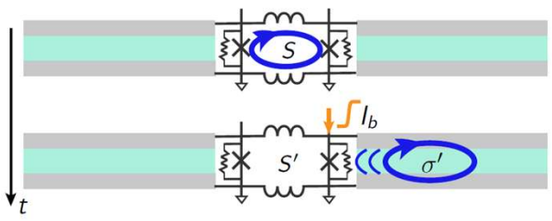

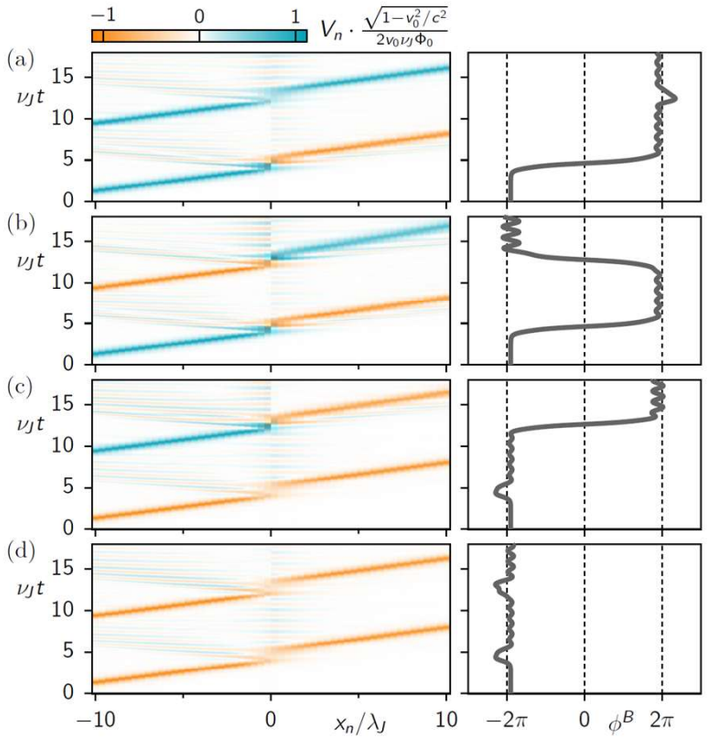

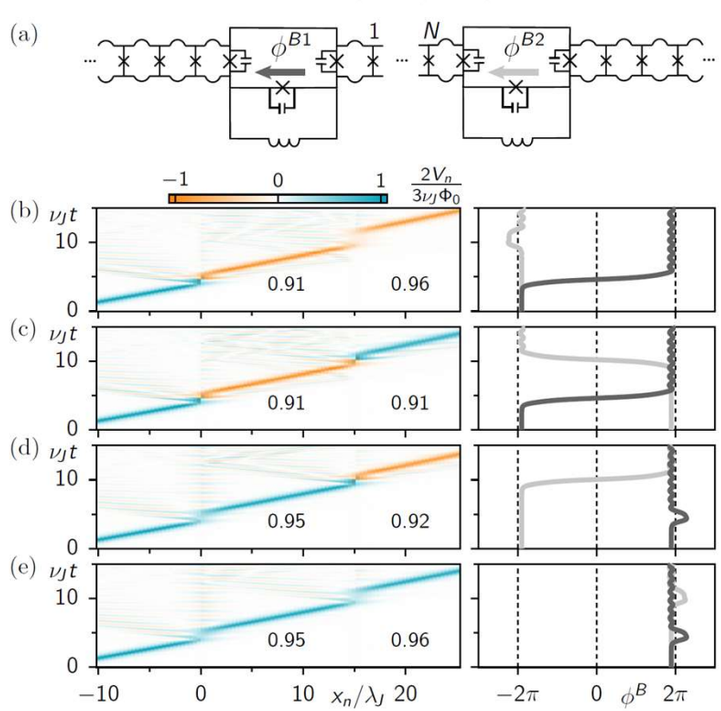

Ballistic Shift Registers, cont.

Characterized margins down to efficiency:

- $\eta_v = 0.6, \eta_E = 0.86, \eta_K = 0.29$

Worst-case efficiency w. optimized parameters:

- $\eta_v = 0.91, \eta_E = 0.95, \eta_K = 0.77$

Two-input, two-output version of BSR.

- Margins are very similar.

Energy-delay product est. at 7×10^{-31} J · s.